Article

The Effect of Magnetized Water on the Fresh and Hardened Properties of Slag/Fly Ash-Based Cementitious Composites

Ozer Sevim [1,*], İlhami Demir [1], Erdinc H. Alakara [2], Selahattin Guzelkucuk [3] and İsmail Raci Bayer [4]

1. Department of Civil Engineering, Kırıkkale University, Kırıkkale 71450, Türkiye
2. Department of Civil Engineering, Tokat Gaziosmanpasa University, Tokat 60150, Türkiye
3. Department of Civil Engineering, Kırsehir Ahi Evran University, Kırsehir 40100, Türkiye
4. Instute of Science, Kırıkkale University, Kırıkkale 71450, Türkiye
* Correspondence: ozersevim@kku.edu.tr; Tel.: +90-318-357-4242

Abstract: The physicochemical structure of the mixing water used in concrete has a significant effect on the physical and mechanical properties of cementitious composites. The studies on the effect of magnetized water (MW) on the properties of FA/BFS-based cementitious composites are still in their infancy. This study explores the effect of MW on the fresh and hardened properties of fly ash (FA)/blast furnace slag (BFS)-based cementitious composites. A total of 22 different mixture groups having FA/BFS (0, 5, 10, 15, 20, and 25%) by weight of cement were produced using tap water (TW) and MW. The fresh-state properties (the initial and final setting times and the consistency) and hardened-state properties (the compressive strength, water absorption properties, and rapid chloride ion permeability test) of produced cementitious composites were investigated. The development of hydration products was analyzed using scanning electron microscopy (SEM) and the mercury intrusion porosimetry (MIP) test. The results reveal that the fresh- and hardened-state properties of cementitious composite samples produced with MW are significantly improved. The properties of the samples utilizing MW showed that FA and BFS could be used at a higher rate for the same target properties in cementitious composites by using MW as mixing water. Using up to 25% FA/BFS in cementitious composites prepared with MW is recommended.

Keywords: magnetized water; fly ash; slag; cementitious composite; fresh properties; hardened properties

1. Introduction

Fly ash (FA) is an industrial by-product retained by electronic filters in the chimneys of coal-fired power plants. FA includes oxides such as Fe_2O_3, CaO, MgO, SO_3, Na_2O, and K_2O, while a significant part of the FA consists of SiO_2 and Al_2O_3 [1–4]. FA particles have a mostly spherical shape and an amorphous structure [3]. The diameter of FA particles ranges from 1 to 150 μm, and about 75% are smaller than 45 μm [1,2,5]. The specific gravity of FA usually varies between 2.1 and 3.0 g/cm^3 [3]. FA is used in many areas, including concrete production, road applications, waste-water treatment, soil stabilization, geopolymer concrete applications, and agricultural applications [6–10]. Concrete production is at the forefront of the field where FA is most widely used. The literature shows that FA can improve the fresh and hardened properties of concrete [11–15]. Blast furnace slag (BFS) is an industrial by-product consisting of silicates and aluminosilicates, which is released during pig iron production in furnaces [16,17]. Residues from the combustion of coke, limestone, iron ore, and other materials construct BFS [18]. The specific gravity of BFS is approximately 2.90, while its unit weight is around 1200–1300 kg/m^3 [16,19]. Studies show that BFS can improve the fresh and hardened properties of concrete [20,21]. In addition, since cement production is responsible for 6–9% of global greenhouse gas emissions [22,23], CO_2 emissions can be significantly reduced by using fly ash and slag in concrete [24,25].

The physicochemical structure of the mixing water used in concrete has a significant effect on the physical and mechanical properties of the concrete, such as workability, compressive strength, flexural strength, water absorption, durability, and permeability [26–29]. Hydrogen bonds between the molecules of water, a polar material, cause clusters. Each water cluster generally contains 100 water molecules at room temperature [26,30]. After the water passes through a particular magnetic field, some changes occur in its molecular structure, and this is called magnetized water (MW). The molecular structure of water passing through a permanent magnetic field has different properties. Danish physicist Hendricks Anton Lorenz discovered this effect in water in the early 1900s [31,32]. The water cluster exposed to the magnetic field breaks up into smaller clusters. In this way, the size and number of water clusters decreases, and the water molecules disperse, as presented in Figure 1 [33–35]. As a result, the activities of water molecules increase [31]. MW differs from tap water (TW) in terms of mechanical, thermodynamic, and electromechanical properties [26]. Due to these properties, MW is used in many applications, such as agricultural, industrial, and medical fields [36].
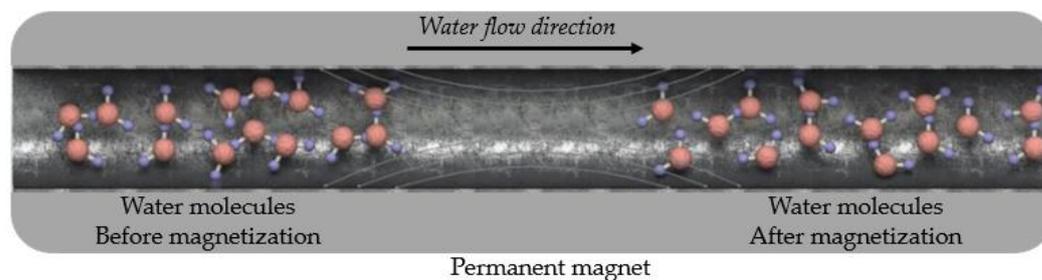

Figure 1. A schematic view of the dispersion of water molecules after passing through the magnetic field. Adapted with permission from reference [32].

MW has a lower surface tension than TW, and the surface tension of MW is measured with a device called a tensiometer [37]. The surface tension of the water significantly affects the hydration process of cement particles. The hydration process first occurs on the surface of the cement particles in a mixture. Thus, a thin layer of hydration products is formed on the cement particles, which prevents the hydration development of the particles [31]. This hinders the strength development of concrete. The use of MW in concrete enables the water molecules to penetrate the cement particles more quickly and improve the hydration of the cement particles. As a result, the mechanical properties of concrete improve significantly [38–47]. Several researchers have explored the properties of cementitious composites that have MW. Su and Wu [30] investigated the effect of MW produced with different magnetic field densities (0.2, 0.4, 0.6, 0.8, 1.2, and 1.35 Tesla) on mortar and concrete samples containing FA. Depending on the strength of the magnetic field, increases in compressive strength and workability were achieved. Su et al. [31] investigated the compressive strength and workability of mortar and concrete samples containing slag, which they prepared using MW. As a result, they determined that MW increased the compressive strengths of the mortar and concrete samples by up to 19 and 23%, respectively. Wei et al. [35] found that MW reduces the early age shrinkage of concrete and increases its compressive and splitting tensile strengths by 29.95 and 16.01%, respectively. Ahmed [37] reported that the concrete samples produced using MW and nano alumina significantly improved the fresh, hardened, and microstructural properties compared to the control samples. Ghorbani et al. [42] investigated the effect of MW on mortar mixtures containing marble dust at different rates (0, 10, 20, 30, and 40%) with the help of a magnet with a magnetic field strength of 0.65 T. The results of this study showed that MW provided an increase of up to 32% in strength. Barham et al. [44] investigated the effect of concrete mixtures containing MW and silica fume on compressive strength and bond strength, and the results showed that MW increased the compressive strength of all mixtures regardless of the silica fume content. Afshin et al. [45] investigated the effect of MW on some properties

of high-strength concrete, such as compressive strength and workability. As a result, the slump values and compressive strength of the mixtures using MW increased by 45 and 18% compared to the control mixtures. Prabakaran et al. [46] investigated the effect of MW on the compressive and tensile strength properties of polypropylene fiber-reinforced concrete, and the use of MW increased the compressive and splitting tensile strengths by 30 and 21%, respectively. Gholhaki et al. [47] reported that MW could significantly improve the hardened properties of self-compacting concrete; the compressive and splitting tensile strengths of the samples prepared using MW increased by 49% and 41%, respectively.

A detailed literature review has shown that studies on the effect of MW on the properties of FA/BFS-based cementitious composites are still in their infancy. Consequently, the present study explores the effect of MW on the fresh and hardened properties of FA/BFS-based cementitious composites. A total of 22 different mixture groups with FA/BFS (0, 5, 10, 15, 20, and 25%) by weight of cement were produced using TW and MW. The fresh-state properties (the initial and final setting times and the consistency) and hardened-state properties (the compressive strength, water absorption properties, and rapid chloride ion permeability test) of produced cementitious composites were investigated. The development of hydration products was analyzed using scanning electron microscopy (SEM) and the mercury intrusion porosimetry (MIP) test.

2. Experimental Program

2.1. Materials

Ordinary Portland cement (OPC) conforming to the EN 197-1 [48] was used in this study. The fly ash (FA) used in this study was Class F (SiO_2 + Al_2O_3 + Fe_2O_3 > 70% and CaO < 10%) FA obtained from the Sugözü Power Plant in Türkiye. The blast furnace slag (BFS) used in the study was obtained from Bolu Cement in Türkiye. The chemical compositions and physical properties of the OPC, FA, and BFS are presented in Table 1. The sand used in this study was the CEN reference sand specified in EN 196-1 [49].

Table 1. The chemical composition and physical properties of OPC, FA, and BFS.

Chemical Composition (%)	OPC	FA	BFS
SiO_2	21.02	57.80	34.82
Al_2O_3	5.38	20.90	17.73
Fe_2O_3	3.22	5.25	0.65
CaO	62.59	7.84	38.22
MgO	1.98	1.78	5.48
Na_2O	0.22	2.19	0.46
K_2O	0.51	1.61	1.51
SO_3	3.11	0.37	0.55
Other elements	1.97	2.26	0.58
Physical properties			
Specific gravity (unitless)	3.18	2.04	2.87
Blaine fineness (cm^2/g)	3356	2945	3925
Loss on ignition	1.58	1.32	1.43

Two types of water were used in the preparation of mortar mixtures. The first is tap water (TW) taken from municipal water, and the second is magnetized water (MW), obtained by passing tap water through a magnetic field. To obtain MW, TW was passed through a specially designed permanent magnet with a length of 250 mm, an outer diameter of 42 mm, and an inner diameter of 20 mm. The strength of this magnet was 0.6 T. According to the mechanism illustrated in Figure 2, the TW was magnetized with the magnet placed between the circulation pump and the water tank. The TW was passed through a permanent magnetic field for 20 min in a closed circuit and then used in mortar production. TW was used in the curing of the mortars.
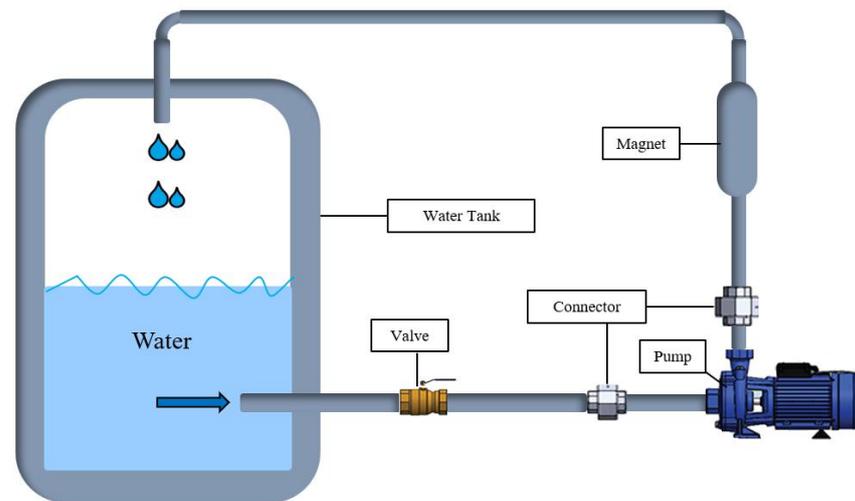
Figure 2. A schematic view of the magnetic water-generating mechanism.

2.2. Mixture Proportions

The cementitious composites were prepared with FA/BFS having replacement ratios of 5, 10, 15, 20, and 25% using MW and TW, as well as the control sample without the FA/BFS. The mixtures were prepared in accordance with EN 196-1 [49]. The mixtures were cast into their molds and kept there until the end of 24 h under humid laboratory conditions. After being removed from their molds, they were moved into a water tank and cured there until the completion of pre-defined total curing periods of 3, 7, and 28 days and then the fresh-state properties (the initial and final setting times and the consistency) and hardened-state properties (the compressive strength, water absorption properties and rapid chloride ion permeability test) of cementitious composites were performed. The mix ratios of the FA/BFS-based cementitious mortars are presented in Table 2.

Table 2. The mixing ratios of FA/BFS-based cementitious mortars.

Mixture ID.	Water Type	Water (g)	FA (%)	BFS (%)	FA (g)	BFS (g)	Cement (g)	Sand (g)
RefTW		225	0	-	0.0	-	450.0	1350
FA5TW		225	5	-	22.5	-	427.5	1350
FA10TW		225	10	-	45.0	-	405.0	1350
FA15TW		225	15	-	67.5	-	382.5	1350
FA20TW		225	20	-	90.0	-	360.0	1350
FA25TW	Tap Water	225	25	-	112.5	-	337.5	1350
BFS5TW		225	-	5	-	22.5	427.5	1350
BFS10TW		225	-	10	-	45.0	405.0	1350
BFS15TW		225	-	15	-	67.5	382.5	1350
BFS20TW		225	-	20	-	90.0	360.0	1350
BFS25TW		225	-	25	-	112.5	337.5	1350
RefMW		225	0	-	0.0	-	450.0	1350
FA5MW		225	5	-	22.5	-	427.5	1350
FA10MW		225	10	-	45.0	-	405.0	1350
FA15MW		225	15	-	67.5	-	382.5	1350
FA20MW		225	20	-	90.0	-	360.0	1350
FA25MW	Magnetized Water	225	25	-	112.5	-	337.5	1350
BFS5MW		225	-	5	-	22.5	427.5	1350
BFS10MW		225	-	10	-	45.0	405.0	1350
BFS15MW		225	-	15	-	67.5	382.5	1350
BFS20MW		225	-	20	-	90.0	360.0	1350
BFS25MW		225	-	25	-	112.5	337.5	1350

2.3. Test Methods

2.3.1. Fresh Properties

The setting time and workability measurements of FA/BFS-based cementitious mortars prepared with TW or MW were performed per EN 196-3 [50]. A mini-slump test determined the workability measurements. While making this measurement, the mortar mixtures that were prepared according to EN 196-1 [49] were poured into the truncated conical mold on the flow table. The mortars were poured into the mold in 2 layers and 25 times rodding in each layer was applied. Subsequently, the truncated conical mold was lifted slowly, and by turning the shaking device, 25 strokes were made in 15 s per EN 12350-3 [51]. After the shaking process, the flow diameters of the mortars in both directions were measured, and the average was taken as the final flow diameter value.

2.3.2. Compressive Strength

The compressive strength of the FA/BFS-based cementitious mortars prepared with TW or MW was determined per EN 196-1 [49]. In this respect, $40 \times 40 \times 160$ mm prismatic samples having different ratios of FA and BFS (0, 5, 10, 15, 20, and 25%) were produced. While performing the compressive strength test, the sample placed in a cross-sectional area of 40×40 mm was loaded with a loading speed of 2.4 kN/s. The average of the compressive strengths of six prismatic samples for each curing age was taken as the final compressive strength value. A UTCM-6431 coded device belonging to the UTEST company was used in the experiments.

2.3.3. Water Absorption

The cubic mortar samples with dimensions of $50 \times 50 \times 50$ mm^3 (width $\times$ height $\times$ length) were used for the water absorption test. This experiment was conducted on three samples for each mixture, and the average result was accepted as the final water absorption value. Water absorption was determined per ASTM C642 [52] for 3-, 7- and 28-day curing periods. The procedure of the experiment was as follows: first, the surface of the samples, which were removed from the water curing, was dried with the help of a towel and weighed (B). Subsequently, the samples were kept in an oven at 100 ± 5 °C for 24 h and weighed again at 20 °C–25 °C (A). Finally, the water absorption values of the cementitious mortars were calculated using Equation (1):

$$\textit{Water absorption percentage} : \left[\frac{B - A}{A} \right] \times 100 \qquad (1)$$

2.3.4. Rapid Chloride Ion Permeability

The rapid chloride ion permeability test (RCPT) of the FA/BFS-based cementitious mortars prepared with TW or MW was performed per ASTM C 1202 [53] for 3-, 7- and 28-day curing periods. For this experiment, Ø100 $\times$ 200 mm cylindrical samples were prepared per EN 196-1 [49] and cured for 3, 7, and 28 days. Before the experiment, these samples were cut in Ø100 $\times$ 50 mm dimensions, and test samples were produced. In this respect, four cylindrical samples were used for each mixture group, and the average result was accepted as the final RCPT value. During the test, the mortar samples were placed in the test cell, one end of which was in contact with a 0.30 M sodium hydroxide (NaOH) solution and the other end with a 3% sodium chloride (NaCl) solution. Mortar samples were exposed to a constant voltage of 60.0 ± 0.1 V for six hours, and the total amount of current passing through each sample was measured in Coulombs © and recorded. The RCPT results were classified from "Negligible" to "High" per ASTM C 1202 [53]. The test device belonging to the Geotechnical Testing Equipment of the RCPT experiment is illustrated in Figure 3.

Figure 3. The RCPT test device.

2.3.5. Mercury Intrusion Porosimetry (MIP)

The pore size distribution of the cementitious composite samples RefTW, RefMW, FA10MW, FA20MW, BFS10MW, and BFS20MW, which were water cured for 7 and 28 days, was characterized by mercury intrusion porosimetry (MIP) test. The Quantachrome Poremaster PM60 test device was used. The MIP measurements were carried out with a device capable of producing pressures up to 414 MPa and a contact angle of 130. Before the measurement, the samples were dried at 50 °C until they reached a constant weight. MIP is widely used to characterize the pore structure of cementitious materials [1,54,55].

2.3.6. Microstructure Analysis

The microstructural properties of RefTW, RefMW, FA10MW, FA20MW, BFS10MW, and BFS20MW, which were water cured for 7 and 28 days, were investigated. The microstructure analyses were investigated with the help of a scanning electron microscope (SEM) using Zeiss EVO 40XP. The SEM analyses were conducted on small samples coated with gold to obtain clear images.

3. Results and Discussion

3.1. Fresh Properties

3.1.1. Setting Characteristics

Figure 4 illustrates the initial setting times of the FA/BFS-based cementitious pastes prepared with TW or MW, together with the error bar illustrating the standard deviation. The results show that the initial setting times of cement pastes produced with MW were longer than those produced with TW. This result is in accordance with the results of the previous study [42]. Figure 4 shows that the initial setting times increased as the FA and BFS replacement ratios increased, regardless of the water type. The results obtained are compatible with the results of previous studies [56–58]. In samples produced with TW or MW, the initial setting times of the FA-based samples were higher than those of the BFS-based samples. This can be attributed to the fact that the specific surface area of BFS is higher than that of FA; thus, it hydrates faster.

Figure 5 illustrates the final setting times of the FA/BFS-based cementitious pastes prepared with TW or MW, together with the error bar illustrating the standard deviation. The results show that the final setting times of cement pastes produced with MW were longer than those produced with TW. This result is in accordance with the results of the previous study [42]. In addition, as the FA and BFS replacement ratios increased, the final setting times also increased regardless of the water type. The results are compatible with

previous studies [56,57]. The final setting times of the FA-based samples were higher than those of the BFS-based samples in all mixture groups.
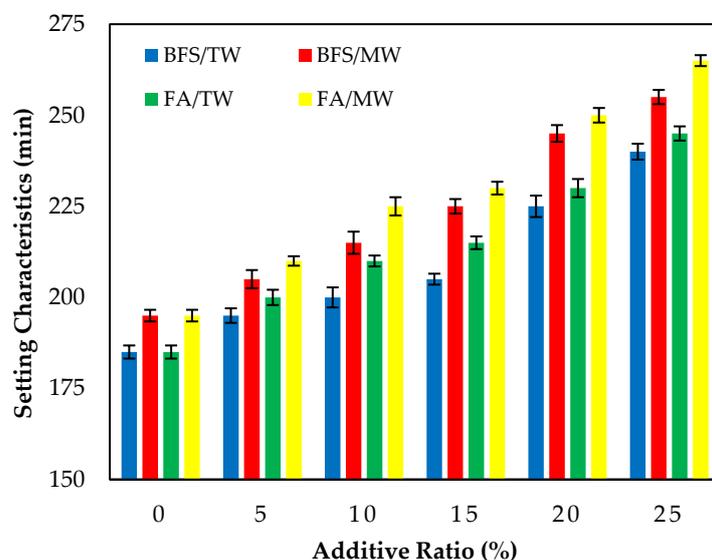

Figure 4. The initial setting time of the FA/BFS-based cementitious pastes.
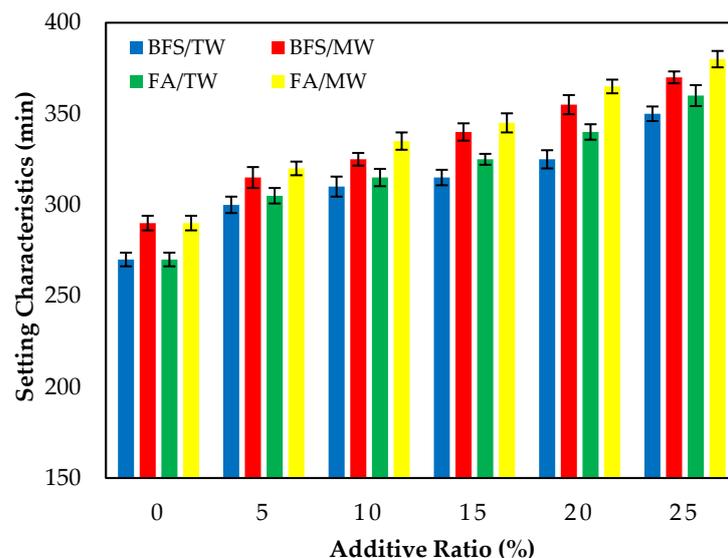

Figure 5. The final setting time of the FA/BFS-based cementitious pastes.

As the replacement ratio increased, the initial and final setting times of the supplementary cementitious materials (SCMs), such as FA and BFS, increased compared to the control samples. This might be attributed to the SCMs, such as FA and BFS, starting the hydration late and delaying the setting times.

3.1.2. Consistency

Figure 6 demonstrates the FA/BFS-based cementitious mortars prepared with TW or MW flow diameters, together with the error bar illustrating the standard deviation. The consistency of fresh cement mortars prepared with MW increased compared to those prepared with TW for both the FA and BFS additives. The results show that the flow diameters increased as the FA replacement ratio increased, regardless of the water type. The spherical morphological feature of FA could explain this [6]. The literature shows that the FA replacement ratio increases the flow diameter of mortar mixtures. Thus, the results in the present study are compatible with the literature [59,60]. The flow diameters of fresh

mortar samples prepared with MW increased by 11.5, 7.1, 10, 6.25, 9.1, and 8.6% compared to those prepared with TW for 0, 5, 10, 15, 20, and 25% FA replacement ratios, respectively. This can be attributed to the water passing through the magnetic field. The water clusters are broken up and separated into smaller water molecules, resulting in a more fluid state of the mortars.
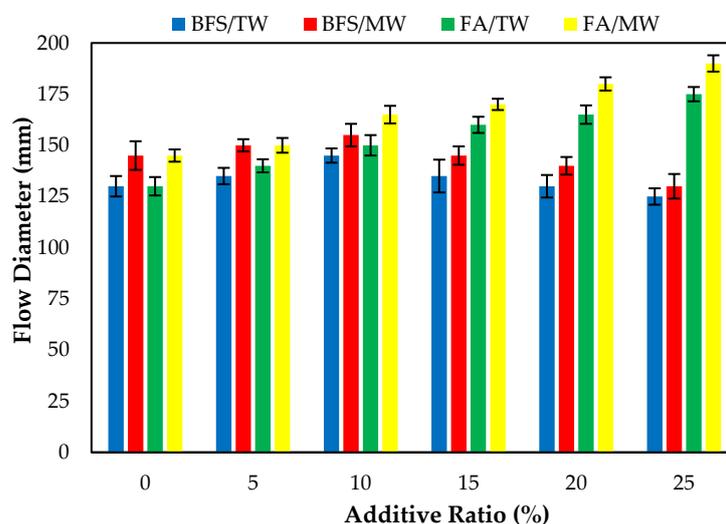

Figure 6. The flow diameters of the FA/BFS-based cementitious mortars.

The flow diameters of the BFS-based mortars produced with TW showed that the flow diameters increased for the 5, 10, and 15% replacement ratios. However, the flow diameter of the 25% BFS-based mortars produced with TW decreased compared to the control mortars produced with TW. This might be attributed to the specific surface area of BFS being higher than cement and FA. After exceeding a certain ratio, the consistency of the BFS-based composites decreased, and thus the flow diameters decreased. The results obtained are similar to the studies conducted on increasing the diffusion diameter of magnetized water [31].

3.2. Compressive Strength

Figure 7 illustrates the compressive strengths of FA/BFS-based cementitious mortars produced with TW or MW for 3-, 7- and 28-day curing periods, together with the error bar illustrating the standard deviation. From Figure 7, the compressive strengths for both FA and BFS-based samples increased with MW. The compressive strengths of the BFS-based mortars were higher than those of FA-based mortars. From Figure 7c, an increase of 8.3–11.1% in the compressive strength of FA-based composites was achieved, while an increase of 10.2–12.5% in the compressive strength of BFS-based composites was achieved with the use of MW. This development seems to align with studies reporting that the mechanical properties of concrete mixes prepared with MW can be improved. The water clusters are broken up into smaller molecules; thus, the activity of the water molecules increases when the water is passed through the magnetic field [33,35]. As a result of this, the binder material hydrates more with magnetized water and significantly contributes to the strength, especially at an early age. Therefore, the compressive strength increased with the use of MW [31,32,42]. Figure 7 shows that the compressive strengths decreased as both the FA and BFS replacement ratios increased, regardless of the water type. This can be attributed to the late completion of hydration of the SCMs, such as FA and BFS, thus reducing their strength at early ages. However, in the case of using BFS, it was observed that these decreases in compressive strength were at lower levels compared to using FA. The reason for this is that the particle size of BFS is smaller than that of FA. The results were similar to those in the literature [12,61]. As a result, it is possible to say that the decreases in the compressive strengths of the SCMs-based cementitious composites at early ages can

be compensated for by using MW. Considering the increase in compressive strength with the use of MW, it has been observed that SCMs such as FA and BFS can be added to the cement at higher replacement rates. In addition, significant savings can be achieved from using cement by evaluating the high number of industrial by-products. Considering that cement production is responsible for approximately 6–9% of greenhouse gas emissions in the world [62–64], it is thought that this rate could be significantly reduced by using a higher amount of SCM.
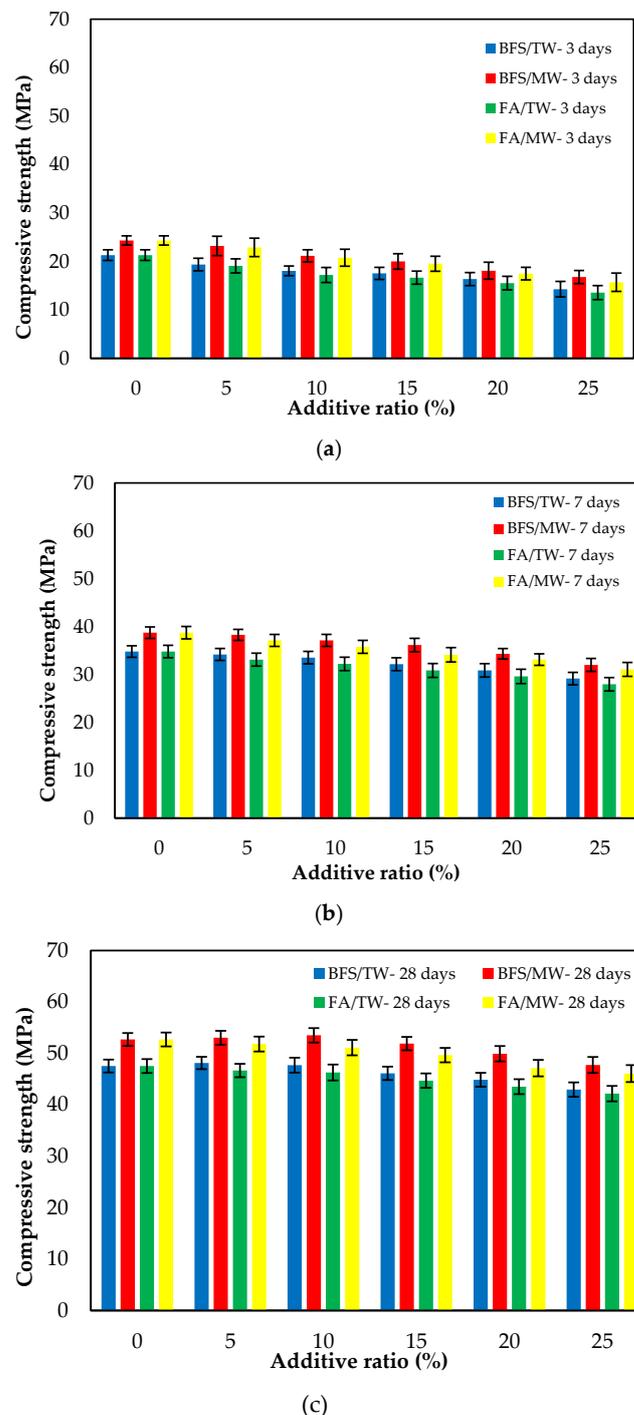
Figure 7. The compressive strengths of the FA/BFS-based cementitious mortars for curing periods of (**a**) 3 days, (**b**) 7 days, and (**c**) 28 days.

3.3. Water Absorption

Figure 8 demonstrates the water absorption of the FA/BFS-based cementitious mortars produced with TW or MW, together with the error bar illustrating the standard deviation. Figure 8 shows that the mortar mixes produced with MW have a lower water absorption than those produced with TW. This can be attributed to the increase in the activity of MW, improving the hydration of the binder and providing a less porous structure of the cement matrix. As the curing age increased, the water absorption decreased. This is because the hydrated elements increased, and the porosity of the mortar matrix decreased. The results show that the water absorption of the BFS-based mortars were at lower levels than the FA-based mortars. The reason for this is that, as in the compressive strength, the particle size of BFS is smaller than that for FA, and it hydrates faster than FA. In this way, BFS creates fewer pores in the mortar matrix compared to FA and reduces water absorption [65]. The 3-, 7- and 28-day water absorption periods showed that the water absorption of the control mixtures increased as both the FA and BFS replacement ratios increased. The main reason for this is the low hydration of FA and BFS at the early ages, the high hydration development in later ages, and the formation of additional hydrates.

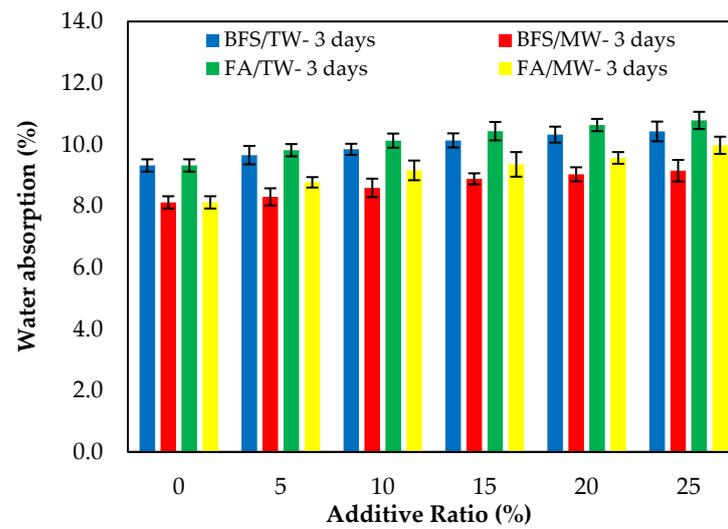### 3.4. Rapid Chloride Ion Permeability

The RCPT results of the FA/BFS-based cementitious mortars produced with TW or MW are presented in Table 3. Table 3 shows that the samples produced with MW have lower RCPT results than those produced with TW at all ages. The chloride ion permeability increased as both FA and BFS replacement ratios increased, regardless of the water type. A comparison of the samples containing FA and BFS shows that the samples containing BFS are more durable in terms of chloride ion permeability than the samples containing FA at all ages, regardless of the water type. A comparison of the chloride ion permeability of the 28-day mortars with those of the 3 and 7-day mortars shows that the voids in the concrete decrease with the effect of hydration reactions in the later ages [1,6]. In addition, the RefMW gave the best results among all mixtures and all ages in terms of the RCPT.

3.5. Mercury Intrusion Porosimetry

Figure 9 illustrates the pore size distribution of the RefTW, RefMW, FA10MW, FA20MW, BFS10MW, and BFS20MW, which were water cured for 7 and 28 days. As the curing age increased, the porosity of each mixture group decreased. In addition, a comparison between the RefTW and RefMW shows that the number of pores can be reduced with the use of MW. The key reason for this is that the surface hardness of the water passed through the magnetic field decreases and the hydration of the binding materials occurs more intensely. The RefMW had a smaller average pore size than the other samples at 7 days, while the FA10MW and FA20MW samples were found to have a smaller average pore size than the RefMW sample at 28 days. The reason for this is that the pozzolanic reaction of FA is forming additional hydrates in later ages and increasing the density of the pores in the matrix [66,67].

3.6. Microstructure Analysis

Figure 10 shows the SEM images of the 7-day water-cured control samples produced with (a) TW and (b) MW. Figure 10b shows that the samples contain more calcium silicate hydrates (C-S-H) than Figure 10a. This can be attributed to MW's low surface tension, thus improving the hydration of the cement. Under these circumstances, the number of hydrated cement particles with MW increases, and more C-S-H is formed.
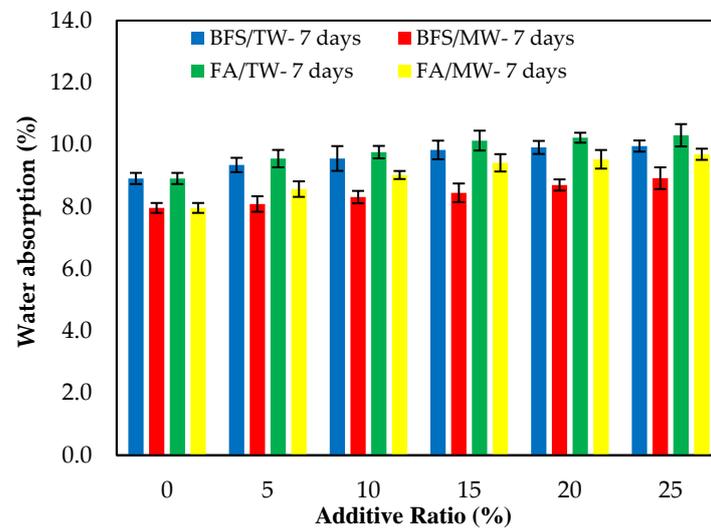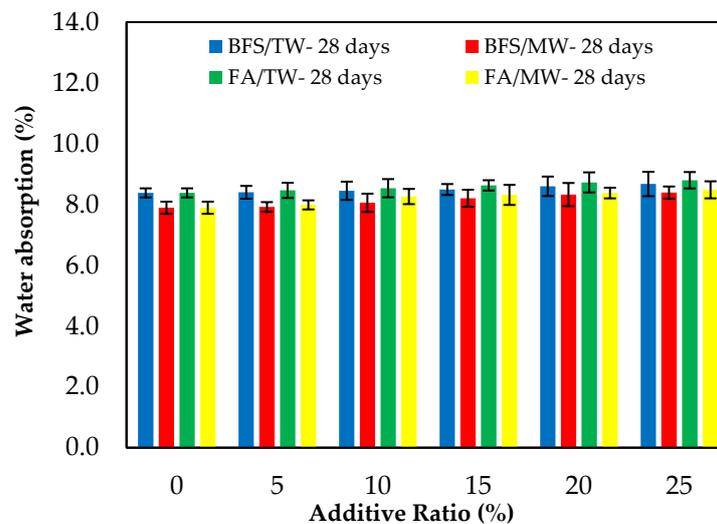
Figure 8. The water absorption of the FA/BFS-based cementitious mortars for the curing periods of (**a**) 3 days, (**b**) 7 days, and (**c**) 28 days.

Table 3. The rapid chloride permeability test results calculated at 3, 7, and 28 days.

Mixture ID.	Rapid Chloride Permeability Test (Coulomb)			Mixture ID.	Rapid Chloride Permeability Test (Coulomb)		
	3-Day	7-Day	28-Day		3-Day	7-Day	28-Day
RefTW	6705	4380	3115	RefTW	6705	4380	3115
FA5TW	7018	4553	3224	BFS5TW	6836	4450	3190
FA10TW	8275	5495	3569	BFS10TW	7955	5205	3340
FA15TW	9018	6108	3771	BFS15TW	8895	5898	3560
FA20TW	10,905	7485	4134	BFS20TW	9865	7095	3895
FA25TW	11,625	7975	4763	BFS25TW	10,965	7565	4255
RefMW	5225	3697	2592	RefMW	5225	3697	2592
FA5MW	5358	3916	2807	BFS5MW	5305	3805	2653
FA10MW	6415	4630	3092	BFS10MW	6253	4350	2875
FA15MW	7132	5093	3255	BFS15MW	6809	4756	3108
FA20MW	8825	5987	3735	BFS20MW	8038	5467	3280
FA25MW	9667	6396	4163	BFS25MW	8955	5957	3976
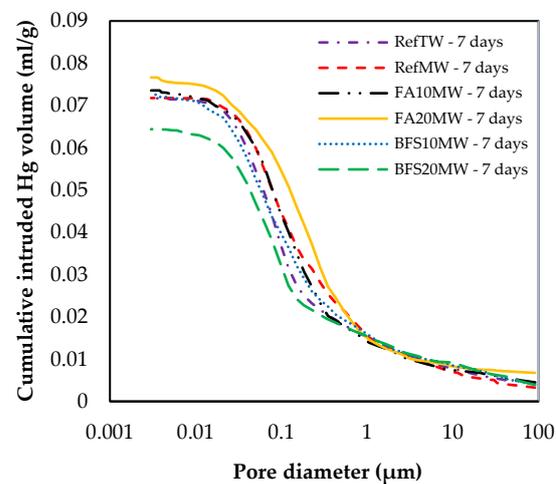
(**a**)
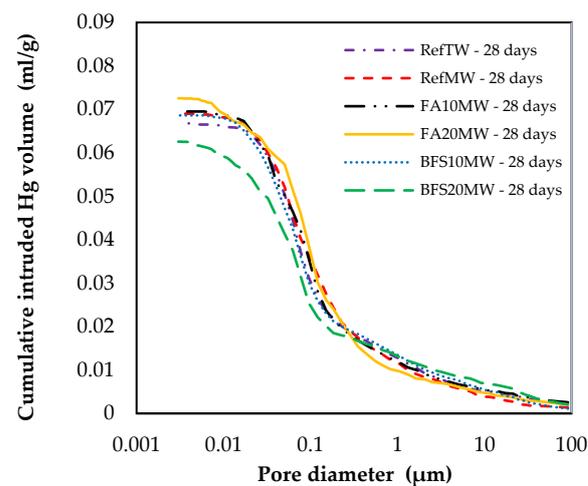
(**b**)

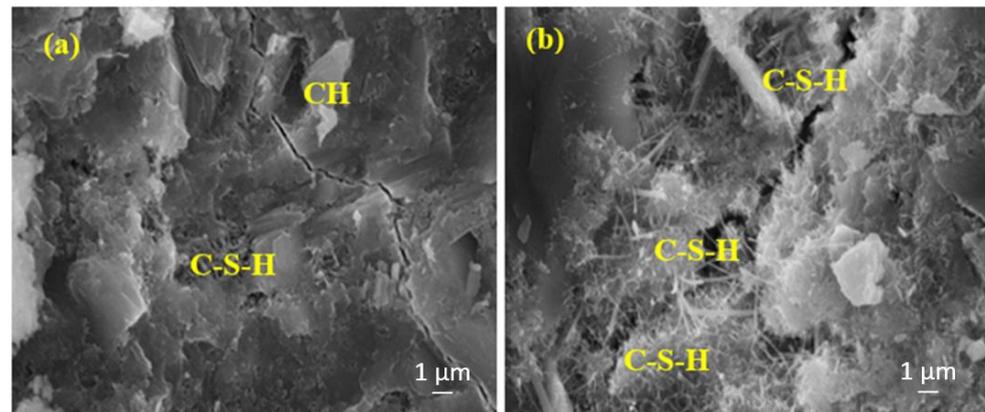**Figure 9.** Changes in size distribution at (**a**) 7 and (**b**) 28 days.

Figure 10. The SEM images of (**a**) RefTW and (**b**) RefMW composites after 7 days of water curing.

Figure 11a shows a more intense C-S-H compared to Figure 11b. This is because Figure 11b contains a higher rate of FA, and the hydration development of FA is lower at the early ages and higher at the later ages.
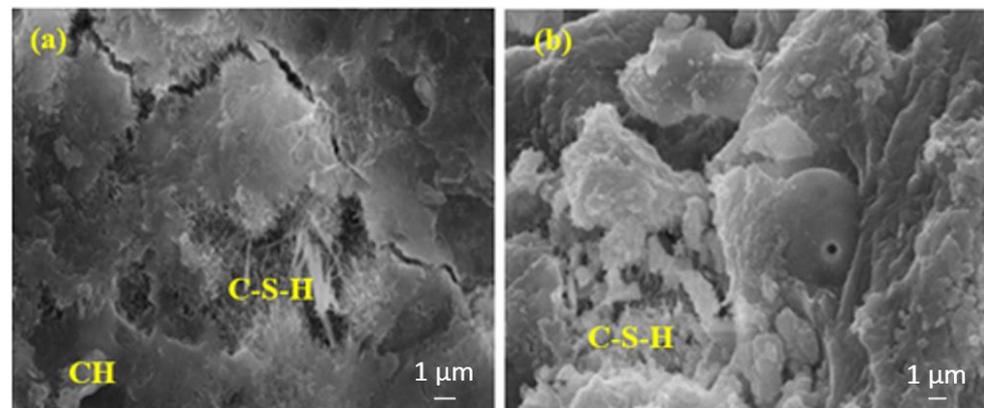

Figure 11. The SEM images of (**a**) FA10MW and (**b**) FA20MW composites after 7 days of water curing.

Figure 12a shows a more intense C-S-H than Figure 12b. From Figure 12a, the calcium hydroxide (CH) can be seen to gradually transform into C-S-H. The CH is more densely packed than the C-S-H in Figure 12b. This is because Figure 12b contains a higher rate of BFS and the hydration development of the BFS is lower at the early ages and higher at the later ages.

The amounts of C-S-H in Figure 13a,b are almost the same. In Figure 14b the amount of C-S-H is slightly more intense than in Figure 14a.
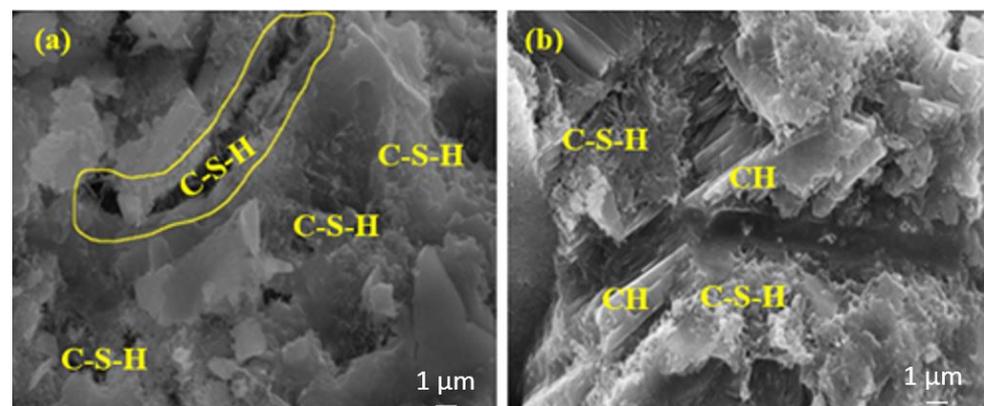

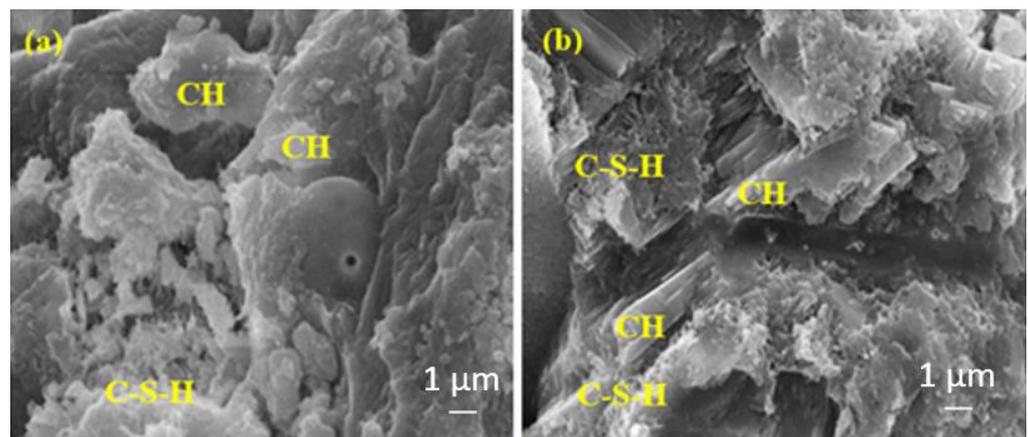**Figure 12.** The SEM images of (**a**) BFS10MW and (**b**) BFS20MW composites after 7 days of water curing.

Figure 13. The SEM images of (**a**) FA20MW and (**b**) BFS20MW composites after 7 days of water curing.
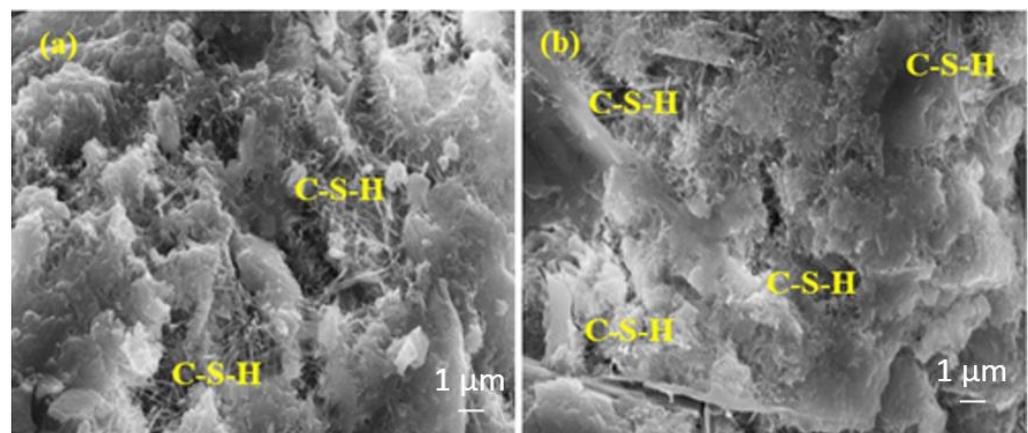

Figure 14. The SEM images of (**a**) RefTW and (**b**) RefMW composites after 28 days of water curing.

Figure 15a shows a more intense C-S-H than Figure 15b. This is because the sample in Figure 15b contains a higher rate of FA, and the hydration development of FA is slower and higher in the later ages.

Figure 16 shows that the amount of C-S-H is approximately the same for both samples; however, the amount of C-S-H in the matrix containing the 10% BFS is slightly higher than the matrix containing the 20% BFS. This is because the sample in Figure 16b contains a higher rate of BFS, and the slower hydration development of the BFS is higher in the later ages.
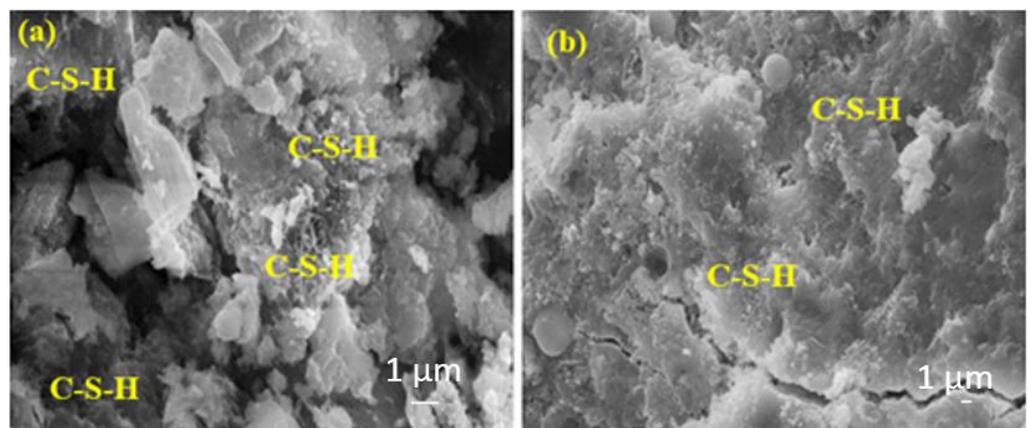

Figure 15. The SEM images of (**a**) FA10MW and (**b**) FA20MW composites after 28 days of water curing.
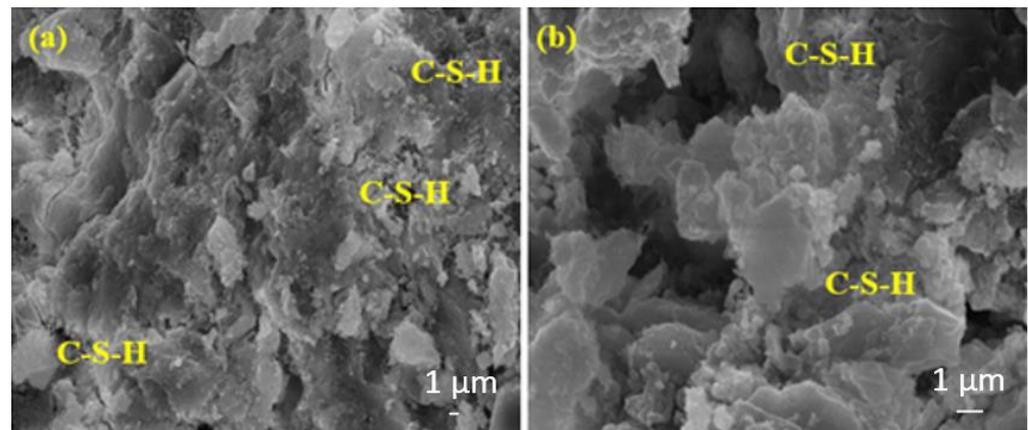
Figure 16. The SEM images of (**a**) BFS10MW and (**b**) BFS20MW composites after 28 days of water curing.

The amount of C-S-H in Figure 17b is high. This can be attributed to the higher hydration rate of BFS compared to FA. It is important to note that the results may vary in different parts of the samples as mortar is heterogeneous.
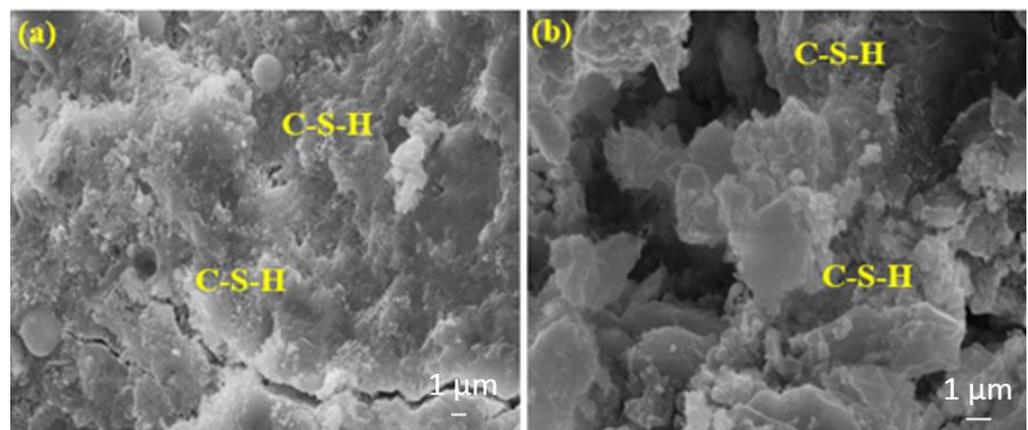

Figure 17. The SEM images of (**a**) FA20MW and (**b**) BFS20MW composites after 28 days of water curing.

4. Conclusions

This study investigates the effect of MW on the fresh and hardened properties of FA/BFS-based cementitious composites. A total of 22 different mixture groups with FA/BFS (0, 5, 10, 15, 20, and 25%) by weight of cement were produced using TW and MW. The fresh-state properties (the initial and final setting times and the consistency) and hardened-state properties (the compressive strength, water absorption properties and rapid chloride ion permeability test) of produced cementitious composites were investigated. The following conclusions can be made based on the findings of this study:

(1) The initial and final setting times of cement pastes produced with MW were longer than those produced with TW. The consistency of fresh cement mortars prepared with MW increased compared to those prepared with TW for both the FA and BFS additives. This can be attributed to the fact that when the water is passed through the magnetic field, the water clusters are broken up and separated into smaller water molecules, resulting in the mortars being more fluid. The flow diameters increased as the FA replacement ratio increased, regardless of the water type;

(2) The compressive strengths for both the FA and BFS-based samples increased with the use of MW. This might be attributed to the binder material hydrating more with the MW;

(3)　The mortar mixes produced with MW have a lower water absorption than those produced with TW. The samples produced with MW have lower RCPT results than those produced with TW at all ages. The chloride ion permeability increased as both the FA and BFS replacement ratios increased, regardless of the water type. This might be attributed to the increase in the activity of MW, improving the hydration of the binder and providing a less porous structure of the cement matrix;

(4)　Using up to 25% FA/BFS in cementitious composites prepared with MW is recommended. Thus, the use of cement will be saved, the amount of CO_2 released to nature will be reduced, and significant contributions will be made in terms of sustainability;

(5)　With the use of MW, the workability of cementitious composites will increase, and it will reduce the use of plasticizer chemicals in cementitious composites; therefore, the cost will decrease;

(6)　It is thought that using MW will provide significant advantages for the sector representatives. Although the initial installation cost of the MW system is seen as high, the installation cost will be met by the future cost savings;

(7)　In further studies, the use of MW on the properties of geopolymers/alkali-activated materials could be investigated. In addition, the effects of MW on shrinkage cracks and the hydration heat of cementitious composites could be examined.

References

1.　Sevim, Ö.; Demir, İ. Optimization of fly ash particle size distribution for cementitious systems with high compactness. *Constr. Build. Mater.* **2019**, *195*, 104–114. [CrossRef]

2.　Kim, T.; Davis, J.M.; Ley, M.T.; Kang, S.; Amrollahi, P. Fly ash particle characterization for predicting concrete compressive strength. *Constr. Build. Mater.* **2018**, *165*, 560–571. [CrossRef]

3.　Ahmaruzzaman, M. A review on the utilization of fly ash. *Prog. Energy Combust. Sci.* **2010**, *36*, 327–363. [CrossRef]

4.　Hemalatha, T.; Ramaswamy, A. A review on fly ash characteristics-Towards promoting high volume utilization in developing sustainable concrete. *J. Clean. Prod.* **2017**, *147*, 546–559. [CrossRef]

5.　Blissett, R.S.; Rowson, N.A. A review of the multi-component utilization of coal fly ash. *Fuel* **2012**, *97*, 1–23. [CrossRef]

6.　Sevim, Ö.; Demir, İ. Physical and permeability properties of cementitious mortars having fly ash with optimized particle size distribution. *Cem. Concr. Compos.* **2019**, *96*, 266–273. [CrossRef]

7.　Tastan, E.O.; Edil, T.B.; Benson, C.H.; Aydilek, A.H. Stabilization of organic soils with fly ash. *J. Geotech. Geoenviron. Eng.* **2011**, *137*, 819–833. [CrossRef]

8.　Basu, M.; Pande, M.; Bhadoria, P.B.S.; Mahapatra, S.C. Potential fly-ash utilization in agriculture: A global review. *Prog. Nat. Sci.* **2009**, *19*, 1173–1186. [CrossRef]

9.　Movilla-Quesada, D.; Muñoz, O.; Raposeiras, A.C.; Castro-Fresno, D. Thermal suspectability analysis of the reuse of fly ash from cellulose industry as contribution filler in bituminous mixtures. *Constr. Build. Mater.* **2018**, *160*, 268–277. [CrossRef]

10.　Rameshwaran, P.M.; Madhavi, T.C. Flexural behaviour of fly ash based geopolymer concrete. *Mater. Today Proc.* **2021**, *46*, 3423–3425. [CrossRef]

11.　Leng, F.; Feng, N.; Lu, X. An experimental study on the properties of resistance to diffusion of chloride ions of fly ash and blast furnace slag concrete. *Cem. Concr. Res.* **2000**, *30*, 989–992. [CrossRef]

12.　Demir, İ.; Güzelkücük, S.; Sevim, Ö. Effects of sulfate on cement mortar with hybrid pozzolan substitution. *Eng. Sci. Technol. Int. J.* **2018**, *21*, 275–283. [CrossRef]

13. Erdoğdu, K.; Türker, P. Effects of fly ash particle size on strength of Portland cement fly ash mortars. *Cem. Concr. Res.* **1998**, *28*, 1217–1222. [CrossRef]
14. Pandian, N.S. Fly ash characterization with reference to geotechnical applications. *J. Indian Inst. Sci.* **2004**, *84*, 189–216.
15. Shaikh, F.U.; Supit, S.W. Compressive strength and durability properties of high volume fly ash (HVFA) concretes containing ultrafine fly ash (UFFA). *Constr. Build. Mater.* **2015**, *82*, 192–205. [CrossRef]
16. Das, B.; Prakash, S.; Reddy, P.S.R.; Misra, V.N. An overview of utilization of slag and sludge from steel industries. *Resour. Conserv. Recycl.* **2007**, *50*, 40–57. [CrossRef]
17. Özbay, E.; Erdemir, M.; Durmuş, H.İ. Utilization and efficiency of ground granulated blast furnace slag on concrete properties—A review. *Constr. Build. Mater.* **2016**, *105*, 423–434. [CrossRef]
18. Shi, C.; Qian, J. High performance cementing materials from industrial slags—A review. *Resour. Conserv. Recycl.* **2000**, *29*, 195–207. [CrossRef]
19. *ACI 233R-03*; Slag Cement in Concrete and Mortar. ACI Committee: Detroit, MI, USA, 2003.
20. Ballim, Y.; Graham, P.C. The effects of supplementary cementing materials in modifying the heat of hydration of concrete. *Mater. Struct.* **2009**, *42*, 803–811. [CrossRef]
21. Gesoğlu, M.; Güneyisi, E.; Özbay, E. Properties of self-compacting concretes made with binary, ternary, and quaternary cementitious blends of fly ash, blast furnace slag and silica fume. *Constr. Build. Mater.* **2009**, *23*, 1847–1854. [CrossRef]
22. Xie, J.F.; Huang, Y.X.; Li, W.W.; Song, X.N.; Xiong, L.; Yu, H.Q. Efficient electrochemical CO_2 reduction on a unique chrysanthemum-like Cu nanoflower electrode and direct observation of carbon deposite. *Electrochim. Acta* **2014**, *139*, 137–144. [CrossRef]
23. Madlool, N.A.; Saidur, R.; Hossain, M.S.; Rahim, N.A. A critical review on energy use and savings in the cement industries. *Renew. Sustain. Energy Rev.* **2011**, *15*, 2042–2060. [CrossRef]
24. Meyer, C. The greening of the concrete industry. *Cem. Concr. Compos.* **2009**, *31*, 601–605. [CrossRef]
25. Sun, Y.; Wang, K.Q.; Lee, H.S. Prediction of compressive strength development for blended cement mortar considering fly ash fineness and replacement ratio. *Constr. Build. Mater.* **2021**, *271*, 121532. [CrossRef]
26. Jouzdani, B.E.; Reisi, M. Effect of magnetized water characteristics on fresh and hardened properties of self-compacting concrete. *Constr. Build. Mater.* **2020**, *242*, 118196. [CrossRef]
27. Felekoğlu, B.; Türkel, S.; Baradan, B. Effect of water/cement ratio on the fresh and hardened properties of self-compacting concrete. *Build. Environ.* **2007**, *42*, 1795–1802. [CrossRef]
28. Hover, K.C. The influence of water on the performance of concrete. *Constr. Build. Mater.* **2011**, *25*, 3003–3013. [CrossRef]
29. Karimipour, A.; Edalati, M.; Brito, J. Influence of magnetized water and water/cement ratio on the properties of untreated coal fine aggregates concrete. *Cem. Concr. Compos.* **2021**, *122*, 104121. [CrossRef]
30. Su, N.; Wu, Y.H. Effect of magnetic field treated water on mortar and concrete containing fly ash. *Cem. Concr. Compos.* **2003**, *25*, 681–688. [CrossRef]
31. Su, N.; Wu, Y.H.; Mar, C.Y. Effect of magnetic water on the engineering properties of concrete containing granulated blast-furnace slag. *Cem. Concr. Res.* **2000**, *30*, 599–605. [CrossRef]
32. Ghorbani, S.; Gholizadeh, M.; Brito, J. Effect of magnetized water on the mechanical and durability properties of concrete block pavers. *Materials* **2018**, *11*, 1647. [CrossRef]
33. Toledo, E.J.L.; Ramalho, T.C.; Magriotis, Z.M. Influence of magnetic field on physical–chemical properties of the liquid water: Insights from experimental and theoretical models. *J. Mol. Struct.* **2008**, *888*, 409–415. [CrossRef]
34. Oleinikova, A.; Smolin, N.; Brovchenko, I. Influence of water clustering on the dynamics of hydration water at the surface of a lysozyme. *Biophys. J.* **2007**, *93*, 2986–3000. [CrossRef] [PubMed]
35. Wei, H.; Wang, Y.; Luo, J. Influence of magnetic water on early-age shrinkage cracking of concrete. *Constr. Build. Mater.* **2017**, *147*, 91–100. [CrossRef]
36. Xiao-Feng, P.; Bo, D. The changes of macroscopic features and microscopic structures of water under influence of magnetic field. *Phys. B Condens. Matter* **2008**, *403*, 3571–3577.
37. Ahmed, H.I. Behavior of magnetic concrete incorporated with Egyptian nano alumina. *Constr. Build. Mater.* **2017**, *150*, 404–408. [CrossRef]
38. Esfahani, A.R.; Reisi, M.; Mohr, B. Magnetized water effect on compressive strength and dosage of superplasticizers and water in self-compacting concrete. *J. Mater. Civ. Eng.* **2018**, *30*, 04018008. [CrossRef]
39. Ghorbani, S.; Tao, Z.; Brito, J.; Tavakkolizadeh, M. Effect of magnetized water on foam stability and compressive strength of foam concrete. *Constr. Build. Mater.* **2019**, *197*, 280–290. [CrossRef]
40. Venkatesh, S.; Jagannathan, P. An experimental study on the effect of magnetized water on mechanical properties of concrete. *IOP Conf. Ser. Mater. Sci. Eng.* **2020**, *912*, 032081. [CrossRef]
41. Abdel-Magid, T.I.M.; Hamdan, R.M.; Abdelgader, A.A.B.; Omer, M.E.A.; Ahmed, N.M.R.A. Effect of magnetized water on workability and compressive strength of concrete. *Procedia Eng.* **2017**, *193*, 494–500. [CrossRef]
42. Ghorbani, S.; Mohammadi-Khatami, M.; Ghorbani, S.; Elmi, A.; Farzan, M.; Soleimani, V.; Negahban, M.; Tam, V.W.Y.; Tavakkolizadeh, M. Effect of magnetized water on the fresh, hardened and durability properties of mortar mixes with marble waste dust as partial replacement of cement. *Constr. Build. Mater.* **2021**, *267*, 121049. [CrossRef]

43. Choi, M.S.; Kim, Y.S.; Kim, J.H.; Kim, J.S.; Kwon, S.H. Effects of an externally imposed electromagnetic field on the formation of a lubrication layer in concrete pumping. *Constr. Build. Mater.* **2014**, *61*, 18–23. [CrossRef]
44. Barham, W.S.; Albiss, B.; Latayfeh, O. Influence of magnetic field treated water on the compressive strength and bond strength of concrete containing silica fume. *J. Build. Eng.* **2021**, *33*, 101544. [CrossRef]
45. Afshin, H.; Gholizadeh, M.; Khorshidi, N. Improving mechanical properties of high strength concrete by magnetic water technology. *Sci. Iran.* **2010**, *17*, 74–79.
46. Prabakaran, E.; Vijayakumar, A.; Rooby, J.; Nithya, M.A. A comparative study of polypropylene fiber reinforced concrete for various mix grades with magnetized water. *Mater. Today Proc.* **2021**, *45*, 123–127. [CrossRef]
47. Gholhaki, M.; Kheyroddin, A.; Hajforoush, M.; Kazemi, M. An investigation on the fresh and hardened properties of self-compacting concrete incorporating magnetic water with various pozzolanic materials. *Constr. Build. Mater.* **2018**, *158*, 173–180. [CrossRef]
48. *TS EN 197-1*; Cement—Part 1: Composition, Specifications and Conformity Criteria for Common Cements. Turkish Standard Institution: Ankara, Turkey, 2012.
49. *TS EN 196-1*; Methods of Testing Cement—Part 1: Determination of Strength. Turkish Standard Institution: Ankara, Turkey, 2016.
50. *TS EN 196-3*; Methods of Testing Cement—Part 3: Determination of Setting Time and Soundness. Turkish Standards Institution: Ankara, Turkey, 2017.
51. *TS EN 12350-5*; Testing Fresh Concrete—Part 5: Flow Table Test. Turkish Standard Institution: Ankara, Turkey, 2019.
52. *ASTM C642-21*; Standard Test Method for Density, Absorption, and Voids in Hardened Concrete. ASTM International: West Conshohocken, PA, USA, 2021.
53. *ASTM C1202-19*; Standard Test Method for Electrical Indication of Concrete's Ability to Resist Chloride Ion Penetration. ASTM International: West Conshohocken, PA, USA, 2019.
54. Diamond, S. Mercury porosimetry: An inappropriate method for the measurement of pore size distributions in cement-based materials. *Cem. Concr. Res.* **2000**, *30*, 1517–1525. [CrossRef]
55. Yu, Z.; Ye, G. The pore structure of cement paste blended with fly ash. *Constr. Build. Mater.* **2013**, *45*, 30–35. [CrossRef]
56. Zhao, H.; Sun, W.; Wu, X.; Gao, B. The properties of the self-compacting concrete with fly ash and ground granulated blast furnace slag mineral admixtures. *J. Clean. Prod.* **2015**, *95*, 66–74. [CrossRef]
57. Brooks, J.J.; Johari, M.A.M.; Mazloom, M. Effect of admixtures on the setting times of high-strength concrete. *Cem. Concr. Compos.* **2000**, *22*, 293–301. [CrossRef]
58. Gesoglu, M.; Ozbay, E. Effects of mineral admixtures on fresh and hardened properties of self-compacting concretes: Binary, ternary and quaternary systems. *Mater. Struct.* **2007**, *40*, 923–937. [CrossRef]
59. Sevim, O.; Baran, M.; Demir, S. Mechanical and physical properties of cementitious composites containing fly ash or slag classified with help of particle size distribution. *Rom. J. Mater.* **2021**, *51*, 67–77.
60. Lee, S.H.; Kim, H.J.; Sakai, E.; Daimon, M. Effect of particle size distribution of fly ash–cement system on the fluidity of cement pastes. *Cem. Concr. Res.* **2003**, *33*, 763–768. [CrossRef]
61. Sevim, O.; Sengul, C.G. Comparison of the influence of silica-rich supplementary cementitious materials on cement mortar composites: Mechanical and microstructural assessment. *Silicon* **2021**, *13*, 1675–1690. [CrossRef]
62. Sevim, O.; Alakara, E.H.; Guzelkucuk, S. Fresh and hardened properties of cementitious composites incorporating firebrick powder from construction and demolition waste. *Buildings* **2023**, *13*, 45. [CrossRef]
63. Wei, J.; Cen, K. Empirical assessing cement CO_2 emissions based on China's economic and social development during 2001–2030. *Sci. Total Environ.* **2019**, *653*, 200–211. [CrossRef]
64. Alhawat, M.; Ashour, A.; Yildirim, G.; Aldemir, A.; Sahmaran, M. Properties of geopolymers sourced from construction and demolition waste: A review. *J. Build. Eng.* **2022**, *50*, 104104. [CrossRef]
65. Giergiczny, Z. Fly ash and slag. *Cem. Concr. Res.* **2019**, *124*, 105826. [CrossRef]
66. Chindaprasirt, P.; Jaturapitakkul, C.; Sinsiri, T. Effect of fly ash fineness on microstructure of blended cement paste. *Constr. Build. Mater.* **2007**, *21*, 1534–1541. [CrossRef]
67. Kim, S.J.; Yang, K.H.; Moon, G.D. Hydration characteristics of low-heat cement substituted by fly ash and limestone powder. *Materials* **2015**, *8*, 5847–5861. [CrossRef]